Analysis of the dynamics of relaxation type oscillation in glycolysis of yeast extracts

Joachim Das and Heinrich-Gustav Busse
Biochemisches Institut in der Medizinischen Fakultät, Dept. Prof. Dr. B. Havsteen, Otto Meyerhof Haus der Christian-Albrechts-Universität Kiel, D-2300 Kiel, Germany

ABSTRACT In yeasts, the glycolysis may display oscillations of its metabolites while it is converting glucose. The dynamics of the oscillations has been investigated in cytoplasmic extracts of yeast under relaxation type conditions by determining the time course of some of the glycolytic metabolites. The compounds of the nucleotide pool have been identified as fast variables and the glucose derivatives as slow variables of the relaxation type. The period of oscillation has been subdivided into four phases which represent prominent parts of the limit cycle in the phase plane of a slow versus a fast variable. From the reaction processes in these phases, a dynamical picture of the mechanisms of oscillations is suggested. Accordingly, the oscillation results from an alternating activity of the fructose bisphosphate and the polysaccharide synthesis, both of which are coupled to glycolysis via the nucleotide pool. The processes in the phases are analyzed by calculating the rates of the reaction steps in the biochemical pathway.

INTRODUCTION

In the glycolytic pathway, the concentrations of its metabolites may oscillate in time. This has been demonstrated in a single yeast cell (1), in suspensions of yeast (2), in tumor cells (3), in unicellular algae (4), in intact organs, e.g. the heart (5), as well as in cell-free extracts of yeast (6), of beef heart (7), of rat sceletal muscle (8), and of insects (9). The literature on such temporal oscillations has already been reviewed (10, 11).

The temporal oscillation in cells or tissues is most often sinusoidal. However, in cell-free extracts, the trace may markedly deviate from a sinusoidal course by displaying spike, rectangular, or saw tooth forms (12, 13). Phase plane diagrams of oscillations disclose some of the internal structures of the reaction systems. In such diagrams, the system path is plotted as a function of two or more of the reactant concentrations. If the oscillation is represented by concentrations of intermediates, it may appear as a nonintersecting closed line because after one period of the oscillation the concentrations recur. In the case of a purely sinusoidal trace in time, circles or ellipses (14) arise. The closed line is known as a limit cycle. Under specific conditions, the limit cycle may deform to display a triangle or a rectangle with smooth edges (15). On the sides of such polyeders, usually one or a few reaction steps in the underlying reaction system dominate the kinetics. Oscillations of the relaxation type belong to this class of limit cycles (16). They are characterized by two kinds of variables, one of which displays fast changes in time and ideally shows a rectangular shape. The other variable changes slowly and has in the ideal case a saw tooth shape. This property allows the division of a period of oscillation into phases from which the dynamics of reaction within a period may be interpreted as in this paper. A model has been devised which within the experimental errors satisfies this purpose. For the observations, the experimental conditions for glycolysis in yeast extracts have been modified to favor oscillations of the relaxation type (17). A limit cycle is obtained from the oscillatory time course of the concentrations of metabolites and possible dynamics in the oscillatory state are discussed. Polysaccharide synthesis as a sink for ATP agrees with the experimental data.

The proteins cyclin (18) and maturation promoting factor (19) also display an oscillatory course of the relaxation type which suggests similarities in the underlying dynamics of the glycolysis and of the cell cycle. Moreover, similarities in the generation of spatial structures may be expected (20). Recently, models on energy transduction, signal transmission (21, 22), and ion pumps

Address correspondence to Dr. Busse, Biochemisches Institut in der Medizinischen Fakultät, Dept. Prof. Dr. B. Havsteen, Olshausenstr. 40 N11, D-2300 Kiel, Germany.

Abbreviations used in this paper: ACA, acetaldehyde; AK, adenylate kinase, myokinase (EC. 2.7.4.3); DHAP, dihydroxyacetone phosphate; F6P, fructose 6-phosphate (Fru-6-P); FBP, fructose 1,6-bisphosphate (Fru-1,6-P_2); G1P, glucose 1-phosphate (Glc-1-P); G6P, glucose 6-phosphate (Glc-6-P); GAP, glyceraldehyde 3-phosphate; GAPDH, glyceraldehyde 3-phosphate dehydrogenase (EC. 1.2.1.12); HEX, hexokinase (EC. 2.7.1.1); PEP, phosphoenolpyruvate; PFK, phosphofructokinase (EC. 2.7.1.11); DPG;1,3PG, 1,3-bisphosphoglycerate; 2PG, 2-phosphoglycerate; 3PG, 3-phosphoglycerate; PGI, phosphoglucose isomerase (EC. 5.3.1.9); PGK, 3-phosphoglycerate kinase (EC. 2.7.2.3); PGM, phosphogluco mutase (EC. 2.7.5.1); PK, pyruvate kinase (EC. 2.7.1.40); PYR, pyruvate; SYN, polysaccharide synthase; UK, uridylate kinase (UMP kinase); Σ, sum of.

0006-3495/91/08/369/11 $2.00

(23) have been discussed in the context of oscillation and glycolysis (24).

MATERIALS AND METHODS

Reagents

Enzymes, substrates, cosubstrates, and metabolites were obtained from Boehringer (Mannheim, FRG) if not stated otherwise. Other chemicals were purchased from Merck (Darmstadt, FRG). All reagents were of high grade quality.

Enzymatic determinations of metabolites

The concentrations of AMP, ADP, and pyruvate (25); ATP (26); DHA, GAP, FBP, and 3-PG (27, 28); F6P and G6P (29, 30); and glucose (29) were determined by enzymatic methods (for minor modifications: see reference 31) in the supernatant of $HClO_4$-precipitated samples of yeast extract. NAD(H) and NADP(H) were measured in the undiluted yeast extract (32). A photometer (model 181; Hitachi Ltd., Tokyo) was used in the optical tests.

Other determinations

The total concentration of proteins in the extract was determined by the method of Biuret (33). The pH value of the extract was measured with a potentiometric electrode (Radiometer, Copenhagen). The optical density of the culture against its medium was determined in a cuvette with an optical path of 10 mm at 640 nm in a photometer (model 181; Hitachi Ltd.). The dry weight of the culture suspension was estimated by weighing on filter plates (type: Selectron BA 83, ø: 50 mm; pore size: 0,2 μm; Schleicher & Schüll, Dassel, FRG) (34).

Preparation of cytoplasmic yeast extracts

Yeast extracts of *Saccharomyces cerevisiae* ATCC 9080 were prepared as published elsewhere (35). Cultures, of which extracts displayed spontaneous oscillations (36), were harvested in the early stationary phase (37) (arrow in Fig. 1 at 16–18 h when glucose was depleted).

Detection of oscillations in extracts

Oscillations of the NADH concentration in yeast extracts were recorded as the absorbance difference at 340 nm (NADH absorption, maximum) and 400 nm (time invariant reference) (38) in a dual wavelength photometer (model DW 2 Aminco; American Instrument Co., Silver Spring, MD).

The glycolytic oscillation was induced by the addition of trehalose to 136–150 mM (Sigma Chemical Co., St. Louis, MO) in a 1-ml aliquot of yeast extract (35). Only extracts, of which the aliquot displayed at least five oscillatory cycles, were kept for further studies.

Samples of extract supplemented with trehalose

Ten ml of yeast extract (protein content: 56 mg/ml) were kept outside the photometer in a glass vessel (volume: 12 ml) at 25°C. The yeast extract from the vial was circulated (30–60 ml/min) by a peristaltic pump (type 113.50; Heidolph Elektro KG, Schwabach, Germany) through a flow cuvette (light path: 3 mm) in the photometer (model DW 2; Aminco). The volume of the silicone tubes and the cuvette was 1.5 ml. The oscillations were induced by the addition of trehalose to 136 mM to the extract and recorded as described above. Samples of 0.2 ml were taken from the glass vessel at defined times with a micropipette (Eppendorf B 315A, 200 μl, Netheler + Hinz GmbH, Hamburg, FRG). The samples were injected into 800 μl of 6% (vol/vol) $HClO_4$ (30), mixed, and centrifuged at maximal speed (centrifuge; Eppendorf, Hamburg, Germany) to remove the precipitated proteins and stored at −20°C (31).

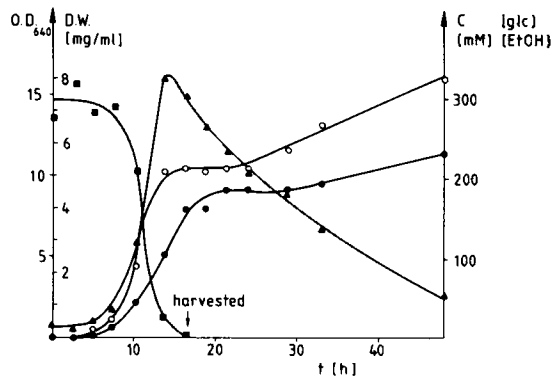

FIGURE 1 Diauxic growth curve of *Saccharomyces cerevisiae* (ATCC 9080). Initial medium: 9.375 g $(NH_4)_2SO_4$, 2.750 g KH_2PO_4, 2.125 g KCl, 0.625 g $MgSO_4 \times 7H_2O$, 0.625 g $CaCl_2 \times 6H_2O$, 12.5 mg $FeCl_3 \times 6H_2O$, 14 mg $MnSO_4 \times H_2O$, 25 g casein hydrolysat, 0.9 g L-tryptophan, 10 g yeast extract (Difco, Detroit, MI), 30 mg ergosterol (Fluka Chem. Corp., Buchs, CH) in 3 ml ethanole, 250 g glucose, 1.25 mg pyridoxamine × HCl, 1.25 mg thiamine × HCl, 0.125 mg D-(+)-biotin, 17.5 mg calcium D(+)pantothenate, 50 mg meso-inositol, 250 ml 0.3 M K-citrate buffer (pH 5.0) supplemented with deionized water to 5 l (24). (- ■ - ■ -) glucose in millimolar; (- ▲ - ▲ -) EtOH in millimolar; (- ● - ● -) optical density (O.D.) at 640 nm with 1 cm light path; (- ○ - ○ -) dry weight (D.W.) in milligrams per milliliter culture medium. At time zero, the culture batch was inoculated with 50 ml of a culture grown overnight.

Sampling of extract supplied continuously with glucose

Eight ml of extract (protein content: 36 mg/ml) was thermostated at 25°C in a titration vessel (type: V516; Radiometer, Copenhagen). The lower conical part of the vessel (diam: ~10 mm), which contained the extract, was positioned in the light path of the photometer (model DW 2; Aminco). Since the lid of the cuvette chamber was dismantled, the photomultiplier had to be protected against the red light (type: 4563; Osram, München, FRG) in the laboratory by a sandwich of two blue glass filters (type: BG13; Schott, Mainz, FRG). During the recording of the absorption difference at 370 and 420 nm (reference), the extract was stirred by a magnetic stirrer (model MS-16B; Toyo) using a magnetic ring (Radiometer, Copenhagen).

The oscillations were induced and sustained by continuous feeding of the extract with ~50 μmol glucose/ml extract/h (or 0.83 μmol/ml/min) (39) from a stock solution of 3 M glucose in 0.1 M potassium phosphate buffer (pH 6.5) by an autoburette (model: ABU12; volume: 250 μl; Radiometer). On the outlet tube of the burette, a precision

syringe (volume: 10 μl; Hamilton, Bonaduz, CH) was mounted, the needle of which was submerged in the extract. A constant rate of feeding was obtained by correction of the glucose input by a computer (model: Micro 16; Digico, Hertfordshire, England) for the loss of volume after a sample had been removed. The samples were removed as described for the trehalose supplemented extracts (31).

Extents of reactions

The concentration C_i of the substance i in a chemical reaction system is related to the extent ξ_j of the reaction j by

$$C_i - C_i^\circ = \mathbf{m}_{ij} \cdot \xi_j, \qquad (1)$$

where C_i^0 is the reference concentration for $\xi_j = 0$. $\mathbf{m}_{ij}$ is the matrix of the stoichiometric coefficients of the reactions. The linear equation system to determine the ξ_j

$$\mathbf{m}_{ki} \cdot \mathbf{m}_{ij}\xi_j = \mathbf{m}_{kl}\,(C_l^\circ - C_l)$$

is obtained by minimizing the sum of squares (40) of the deviation of each equation in the system (1) from zero by a given set of ξ_j. (If an index appears twice in a term of the above equations, then the sum has to be taken over the index.) The equation system still gives a result for the ξ_j if some concentrations C_i are considered to be insignificant (i.e., some rows of m_{ij} are deleted). The computation was performed on a Digital Equipment Corp. (Maynard, MA) PDP 10 with the program system MLAB (41).

RESULTS

Trehalose-induced oscillations

Glycolysis in an extract of yeast was induced by the addition of 136 mM trehalose to determine which of the reactions of the glycolytic pathway run under the oscillatory conditions close to their chemical equilibrium. This approach was chosen because it is less laborious than the glucose injection technique (see Methods). Moreover, many periods without significant changes in shape or damping of the amplitude are obtained. This is true before, and even after, samples have been withdrawn (see Fig. 2). The time course of the components of the adenine nucleotide pool: AMP, ADP, and ATP within the sampling range is plotted in Fig. 3 *c*. The sum, Σ, of the adenine nucleotides remains constant within the sampling range. The concentration of ADP changes surprisingly to only slightly higher values in the narrow time range, in which AMP and ATP are interconverted. The values of the nucleotide concentrations scaled to their constant sum Σ = [AMP] + [ADP] + [ATP] are read for the samples in the phase plane diagram (Fig. 3 *d*). Because the myokinase (AK) catalyzed reaction, due to the high enzymatic activity, remains close to its equilibrium, the mass action law K_{AK} = [ADP]²/[AMP]/[ATP] may be assumed to be valid. If the mass action law and the sum, Σ, are valid for the adenine nucleotide concentrations, then their concentrations should form

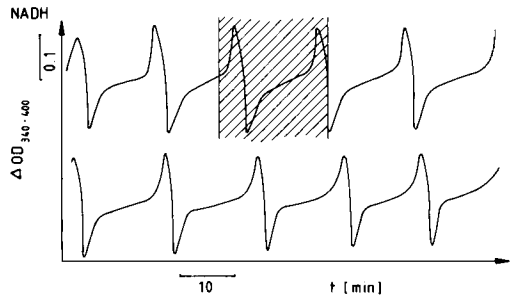

FIGURE 2 NADH-oscillation of an undiluted yeast extract (protein: 56 mg/ml) supplemented with trehalose (136 mM). Recorded is the optical density difference ΔOD between 340 nm and 400 nm as a function of time at 25°C in a flow through cuvette of 3 mm light path. The time range is marked by hatched lines during which 24 samples of 200 μl were withdrawn for further analysis (see Fig. 3). Initial volume of extract in the device: 10 ml. The lower train continues the upper one.

sectors of ellipses in the phase plane as it is seen in Fig. 3 *d* (42). The concentration of ADP reaches its maximal value when [AMP] = [ATP] (42). In the transition ranges (Fig. 3 *c*), the occurrence of the maxima in the concentration of ADP may be explained with the aid of Fig. 3 *d* since when the equilibrium line is followed, e.g., from the low to the high ATP levels, a maximal concentration value for ADP is passed. This supports the assumption that the adenine nucleotide system is operating close to its equilibrium. The time course of [NADH], [F6P], and [G6P] are shown in Figs. 3, *a* and *b* for comparison.

The phase plane representation of [F6P] vs. [G6P] (Fig. 4 *a*) is a typical example of a reaction operating close to its chemical equilibrium: [F6P]/[G6P] = 0.28. The plot of [FBP] vs. [G6P] shows an example of a reaction operating far from equilibrium (Fig. 4 *b*, phosphofructokinase catalyzed reaction), in which case the curve connecting the points does not point toward the origin. This shows that [G6P] and [FBP] are 180° out of phase. Phase plane plots for the reactions of FBP-aldolase and triosephosphate isomerase indicate that they catalyze reactions close to their chemical equilibrium.

Experiments were carried out to optimize the conditions for relaxation type oscillations in extracts supplemented with trehalose. Extracts diluted by a factor greater than 2 with buffer approximated better to the relaxation shape (35). However, the time needed to complete one period also increased. Extracts, in which the glucose supply from trehalose was replaced by an equivalent glucose injection, showed also oscillations of the relaxation type on dilution.

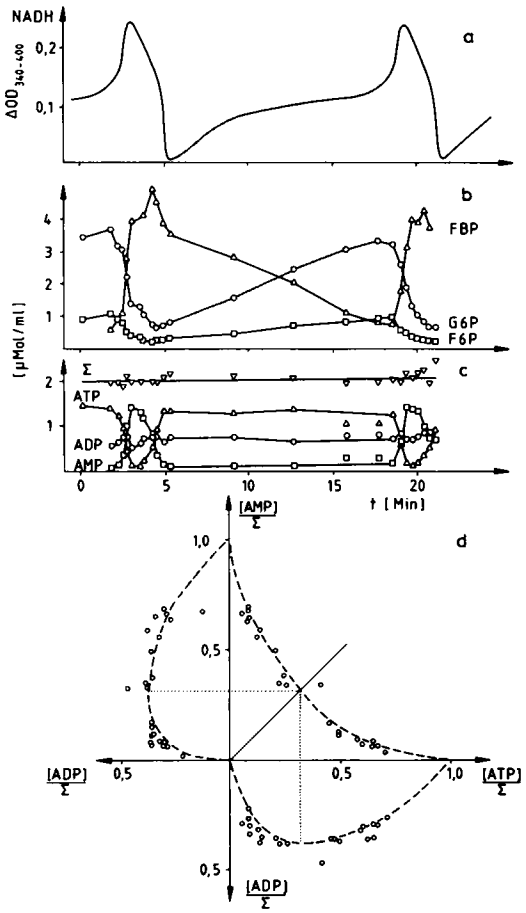

FIGURE 3 Course of concentration of metabolites of glycolysis during a period. (*a*) The record of the optical density of NADH is part of the NADH trace of Fig. 2. The time interval displayed is marked in Fig. 2. (*b*) Time course of the concentration of the intermediates -△-△-FBP, -○-○-G6P, and -□-□-F6P. (*c*) Time course of the concentrations of the adenosine nucleotides -□-□-AMP; -○-○-ADP; -△-△-ATP; and their sum -▽-▽-Σ = [AMP] + [ADP] + [ATP]. (*d*) Phase plane of the adenine nucleotide pool. The nucleotide concentrations are normalized to their constant sum Σ = [AMP] + [ADP] + [ATP]. The estimated arcs of ellipses are drawn with dashed lines. The thin line at 45° is an axis of symmetry. The dotted lines mark the maximal concentration of ADP, at which the concentration of ATP and AMP are equal.

Oscillations of relaxation type induced by continuous injection of glucose

In Fig. 5 *b*, [G6P] and [FBP] demonstrate the typical slow variation of an oscillation of relaxation type. During a phase (I or III) of the period, they steadily increase or decrease to a definite level and then suddenly they enter a second phase in which they decrease or increase continuously to a certain level. The [NADH], [AMP], and [ATP] display the typical shape of fast variables which is characterized by four phases, i.e., a high and low level phase (I and III in Fig. 5), in which the system stays most of the time, and a steplike switch upward or downward (II and IV in Fig. 5) between the two levels. The instants, at which the switching occurs, coincide with those at which the slow variables change their slope.

In general, the time courses of the metabolite concentrations display a pattern similar to the one observed during the trehalose-induced oscillations in Fig. 3. However, they may differ in the levels of FBP and DHAP at the end of a period which might not return to their initial values (see Fig. 5 *b*). Under such conditions FBP and its triose phosphates may accumulate during each cycle and the oscillation is observed to stop after a few cycles. The glucose concentration (Fig. 5 *b*) is determined to ~0.25 μmol/ml during the phase of low ATP concentration but otherwise drops below 0.05 μmol/ml. The sensitivity of the determination is ±0.05 μmol/ml. However, the values of 0.25 μmol/ml may be too high, because high concentrations of some of its derivatives may interfere. Because glucose is not accumulated within a period, the amount of added glucose must be metabolized. In contrast to the pattern in Fig. 3 *c*, neither [ATP] nor [AMP] approach in the experiment of Fig. 5 *b* values close to zero in the slowly varying phase (I), whereas the [ADP] remains nearly constant. In phase II (fast NADH-rise), ATP (0.75), AMP (0.75), G6P (1.3), F6P (0.35), FBP (1.6), DHAP (0.25) change their concentrations (difference given in parentheses in micromoles per milliliter) within a brief time span. The sum of the changes in concentration of G6P and F6P (1.65 μmol/ml) is within the expected experimental error equal to the sum of those of FBP and half of the DHAP (1.7 μmol/ml). GAP values may be neglected compared with the high DHAP values. In the phase IV (fast NADH decline), the change in the concentration of FBP is ~0.5 μmol/ml, whereas neither G6P nor F6P change their concentrations significantly. The rate of increase of G6P and F6P is 0.37 μmol/ml/min and 0.09 μmol/ml/min, respectively, in the slowly varying phase I. Their sum, 0.46 μmol/ml/min, is approximately half of the injection rate 0.83 μmol/ml/min. In the other slow varying phase III, the decrease of G6P is 0.6 μmol/ml/min. The values for FBP in the two phases (I and III) are −0.24 μmol/ml/min and 0.72 μmol/ml/min, respectively, and for DHAP −0.07 and 0.4 μmol/ml/min, respectively.

The phase plane, in which ATP is plotted against NADH (see Fig. 5 *c*), displays a curved relationship between these variables indicating that ATP and NADH are quite strongly coupled and that both are variables of the fast type.

The rate of glucose input was optimized, beginning

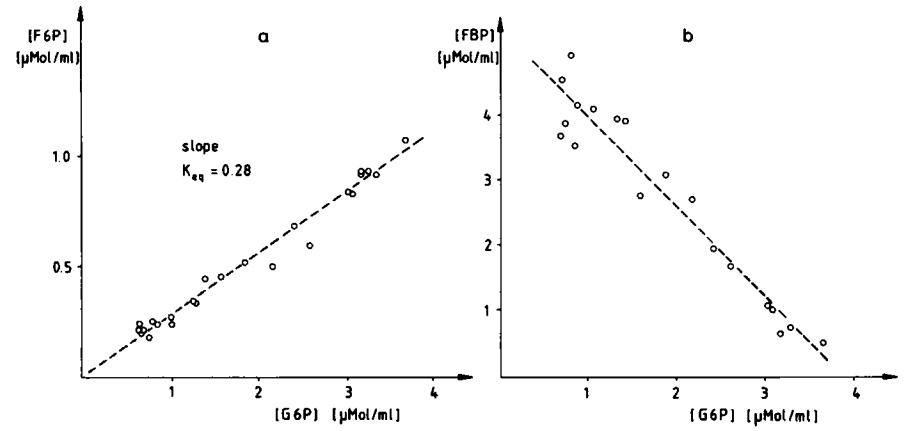

FIGURE 4 (*a*) Phase plane of [F6P] vs. [G6P]. The slope of the line is the equilibrium constant for the isomerization of F6P and G6P; $K_{eq} = 0.28$. (*b*) Phase plane of [FBP] vs. [G6P]. The slope of the line is −1.35. It does not represent an equilibrium constant. Dashed straight lines are drawn to visualize the relationship.

from literature values (39) to gain as many cycles as possible without loss of the relaxation type of the trace. It was noticed that an increase in the rate of stirring decreases the number of cycles in the oscillatory train. However, stirring was necessary since a spatial distribution of glucose could lead to inhomogeneities in the metabolite concentrations (20). Whereas in the experiment of Fig. 2 the rate of glucose supply from trehalose is fixed but unknown, in this experiment the glucose input can be varied in a controlled fashion.

Extent of reactions

The extents of reactions may be obtained from the given concentrations of metabolites by the method outlined (see Methods). Assuming that glucose is converted in the glycolytic pathway to ethanol and CO_2, and that the generated ATP is consumed by formation of a polysaccharide (43–45) (as in the case of the synthesis of glycogen), the computation defines classes of reactions, which move simultaneously. In the lower part of the pathway from glyceraldehyde 3-phosphate to ethanol, all reactions convert the metabolites at nearly the same rate. Hence, the progress of one reaction may be regarded as a representative of its class. In this case, the reaction catalyzed by pyruvate kinase was selected since in the literature it has been considered as a regulating enzyme (10). The simultaneous reaction progress originates from the conservation of NAD in the NADH/NAD^+ loop which forces the amount of substrate entering the loop via the glyceraldehyde 3-phosphate dehydrogenase reaction to leave it simultaneously via the alcohol dehydrogenase reaction.

Moreover, within a pool of reactions which run close to their equilibria, the extents of reactions are related. The metabolization through such a pathway is mainly characterized by the reactions which regulate the flow between the pools of equilibrated reactions. In the tentative scheme of Fig. 6, these reactions are: (*a*) the polysaccharide synthetase reaction, (*b*) the phosphofructokinase reaction, (*c*) the pyruvate kinase reaction for the lower part of the pathway, and (*d*) the reaction simulating the glucose injection. The time courses of these extents of reaction differ significantly (see Fig. 7). Whereas the phosphofructokinase reaction only seems to be activated in phase III (high [NADH]), the pyruvate kinase reaction is always active but especially so in phase III (high [NADH]) (44). The opposite seems to be true for the polysaccharide synthetase reaction. After one period from $t = 0$ to $t = 11$ min (Fig. 7), the pyruvate kinase catalyzed reaction has advanced to the same extent as the glucose injection, i.e., 50% of the glucose injected have been converted to ethanol and CO_2 (44), the other 50% are incorporated either into the polysaccharide (30%) or FBP (70%) because FBP is accumulated in this experiment. The sum of the extents of reaction of the synthetase reaction and the phosphofructokinase reaction equals the extent of the glucose injection because glucose should have been converted by either one or both enzymes.

Phase plane of the limit cycle

A graph of a slow versus a fast variable of a relaxation oscillation yields a closed curve, the limit cycle, because after the elapse of a certain period, both of the variables resume their initial values. A plot of [G6P] as a slow

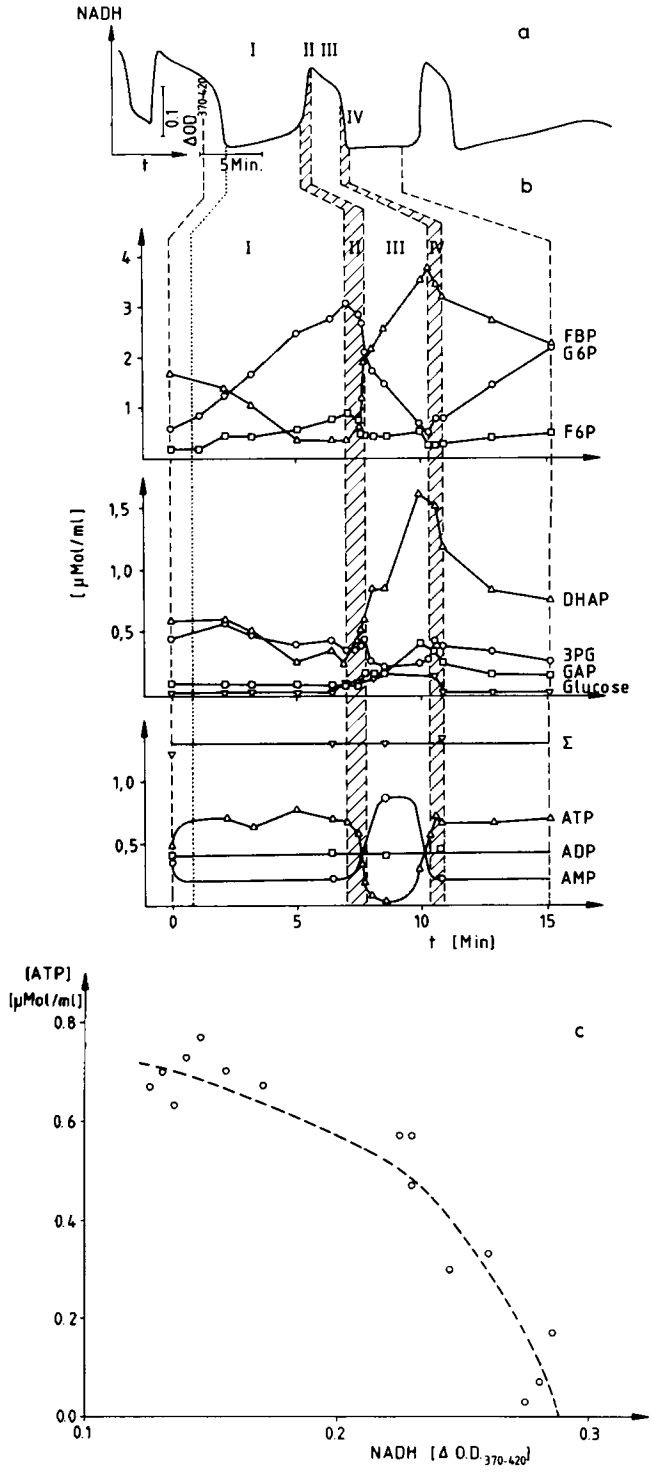

FIGURE 5 (*a*) Time course of an oscillation of the relaxation type. The optical density difference of NADH was recorded in a dual-wavelength mode at 370 and 420 nm as reference. The cytoplasmic extract was diluted by a factor 2 by phosphate buffer (0.1 M; pH = 6.5) to yield a protein concentration of 36 mg/ml. Glucose was fed at a rate of ~50 μmol/ml/h. The time range in which the 18 samples were taken is marked by the outer vertical dashed lines and magnified in the following diagrams. (*b*) Time course of glycolytic metabolites during an oscillation of the relaxation type. Experimental values are connected by a line. The name of the metabolite is given at the right end of the curve. The stepwise increase (at ~7.5 min) and decrease (at ~10.5 min) in the concentration of NADH (*shaded areas*) reflect fast concentration changes in the adenosine nucleotides. The phases of a period of the relaxation type are marked I–IV (see Fig. 8). (*c*) Phase plane diagram of [ATP] and [NADH]. The [NADH] is given in optical density units (see Fig. 2). The dashed line is drawn to visualize the relationship.

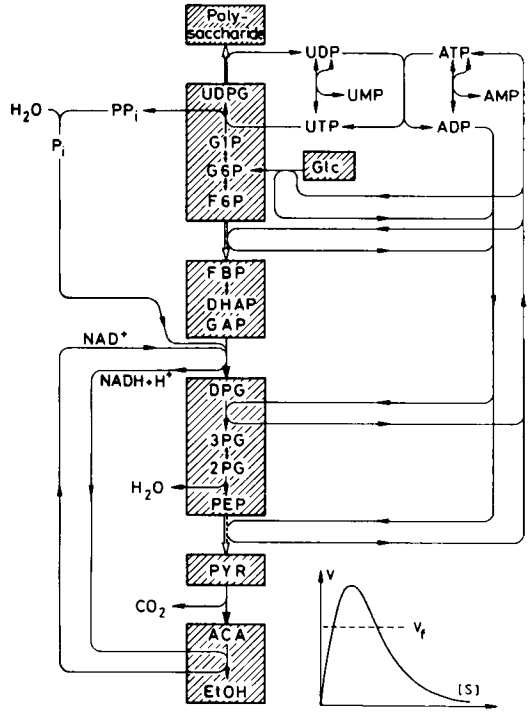

FIGURE 6 Scheme of glucose utilization to synthesize a polysaccharide. Intermediates of reactions which remain close to their chemical equilibrium are surrounded by a box to indicate their interconvertability. The loops connecting nucleotides and dinucleotides of the network are drawn on the left and right side of the pathway. The loop of inorganic phosphate of the pathway is probably detached from the regulation by the relatively high concentration of phosphate in the buffer. The lower left insert gives the typical relation between the activity V and the concentration [S] for the reaction of a substrate-inhibited enzyme. It shows that two substrate concentrations yield the same predefined activity V_f. The enzyme PFK would show substrate inhibition of this kind if [S] = [ATP].

variable against [ATP] as a fast variable would disclose the limit cycle for the glycolytic pathway (see Fig. 8). The four phases of the fast variable are seen more clearly on the limit cycle. They can be identified by marking the two points at which the tangent of the limit cycle is horizontal and the two points at which it is

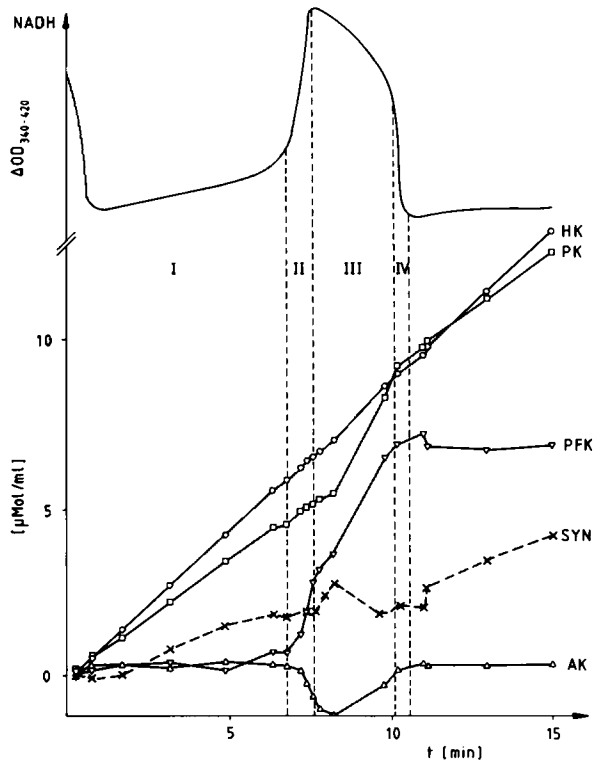

FIGURE 7 Extent of reactions of the rate determining reaction steps in glycolysis calculated from measured metabolite concentrations for: (- □ - □ -) pyruvate kinase (PK); (- ▽ - ▽ -) phosphofructokinase (PFK); (- × - × -) polysaccharide synthase (SYN); (- △ - △ -) adenylate kinase (AK); (- ○—○ -) hexokinase (HK). For orientation, the NADH record has been drawn on top of the diagram.

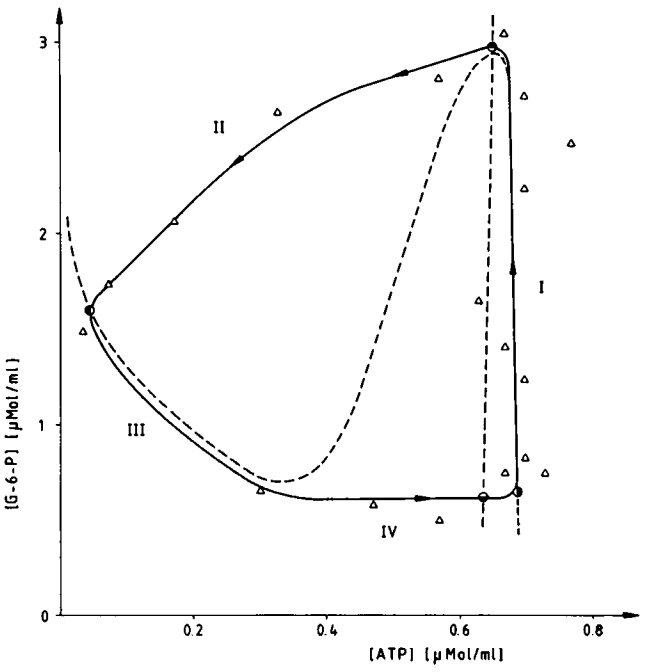

FIGURE 8 Limit cycle in the phase plane of [G6P] vs. [ATP]. A closed curve has been drawn through the experimental points to show the likely position of the limit cycle. The points at which the tangent to this curve is either horizontal or vertical have been marked by ◒, ◑. The two tentative isoclines or nullclines (*dashed lines*) which intersect the limit cycle at the marked points indicate concentration sets (i.e., the graphs) at which the time change in [ATP], [G6P], respectively, is zero. They are the functions in the differential equation system describing the dynamics. The four major phases of the limit cycle have been labelled I–IV.

vertical (see Fig. 8). At these points, the two characteristic isoclines (see Fig. 8) intersect the limit cycle. The points having a vertical tangent are the beginning of the low (I) or high (III) NADH phase (see Fig. 8). The phase ends where the isocline, which runs close to the limit cycle, leaves the latter. The parts of the limit cycle between the two phases correspond to the fast upward and downward steps in the NADH trace (Fig. 5 *a*).

DISCUSSION

Nonsinusoidal oscillations may be used to analyze the dynamics of the oscillatory state of glycolysis. Oscillations of a relaxation type permit the partition of the dynamics into subprocesses which can be studied separately. Models of chemical reaction systems displaying relaxation-type oscillations have already been examined (16). Also, in glycolysis such oscillations have been shown (15). The basic reaction scheme of glycolysis is well known. However, the regulation of the glycolytic pathway under different conditions of energy demand and substrate supply is still a matter of discussion (46). An identification of the regulated steps in glycolysis is essential for the analysis of the oscillatory state. Hence, the first goal in the analysis of the dynamics is to locate the enzymatic steps, which operate close to equilibrium. Because of the law of mass action, the concentrations of the reactants of such steps are closely coupled. In Fig. 6, the intermediates are summarized which are believed to be in equilibrium.

Pools of metabolites

We have verified that the phosphoglucoisomerase, aldolase, and triosephosphate isomerase catalyzed reactions remain close to their chemical equilibrium, as the law of mass action demands. Compounds, which can be interconverted by reactions at or close to their chemical equilibrium, form a pool. The pools are separated by nonequilibrated reactions. The hexosemonophosphates

(G1P, G6P, F6P) and the metabolites (Glc, UDP-Glc) form a pool of compounds in this sense. The size of the pool P is the sum of its components: e.g., P = [G6P] + [F6P] + [G1P] + [Glc] + [UDP-Glc]. Some concentrations, e.g., those of G1P and Glc, remain well below that of G6P. Therefore, the pool size can be estimated from its dominating substance. For example, because F6P = 0.3 × [G6P] at equilibrium, the pool size is P = 1.3 [G6P] at high [G6P]. In the same way, FBP and 3-phosphoglycerate may be used to characterize their pools because [DHAP], [GAP], or pyruvate may under the experimental conditions be less accurate to determine enzymatically. Whereas the size of the pools mentioned above varies with time, the nucleotide pools do not.

An essential reaction in this pool is the myokinase-catalyzed adenine nucleotide interconversion (see Fig. 3 *d*) ATP + AMP $\rightleftharpoons$ 2 ADP which keeps the adenine nucleotide pool at equilibrium. The sum of all adenine nucleotide concentrations Σ = [AMP] + [ADP] + [ATP] should remain constant according to our measurements. Hence, it may be assumed that de novo synthesis and degradation are inactive in the time range of the experiment. The two constraints (law of mass action, mass conservation) on the three adenine nucleotide concentrations imply that given one of the concentrations (e.g., ATP or AMP), both of the others are computable from the diagram in Fig. 3 *d*. Moreover, the diagram verifies that the reaction runs close to its equilibrium since the experimental data fall on the elliptic arcs calculated from the above constraints (42). The uridinephosphates have been treated similarly with the exception that UDP-Glc had to be included in their sum. The uridine- and adenine nucleotide pools are coupled by a nucleotide phosphotransferase (47). Hence, at equilibrium the ratio of [UTP]/[UDP] is given by that of [ATP]/[ADP].

Where [AMP] = [ATP], i.e., where the two curves in Fig. 3 and Fig. 5 intersect, [ADP] reaches its maximal value (see Fig. 3 *c*). In the NADH trace of Fig. 3 and 5, these points mark the end of the fast-rising NADH step and the start of the fast-decreasing NADH step. Because the concentrations of ATP and NADH move in concert in the phase of fast change (Fig. 5 *c*), it is likely that they are related via the glycerate 3-phosphate dehydrogenase reaction.

Dynamics in the phases of the relaxation oscillation

The key to the dynamics in the oscillatory state is the kinetics of phosphofructokinase. The reaction runs far from its chemical equilibrium which is on the FBP side. Its rate is known to be regulated by AMP and ATP. The origin of the oscillatory capability of PFK may be explained by its inhibition at the increasing levels of substrate ATP (48, 49) if the effects of AMP on its rate are neglected. The inset in Fig. 6 illustrates that under stationary conditions with a constant glucose input V_{in} there should be a constant turnover rate $V_f = V_{in}/2$ for PFK (f = flux). Unfortunately, the substrate inhibition allows two concentrations of ATP to reach V_f, one at a low [ATP] value, which is stable, and one at a higher [ATP] which is unstable. In the unstable range, a mean V_f can be obtained by a turnover lower than V_f, which lasts for some time but is compensated by a rate higher than V_f for a succeeding period. The process appears as an oscillation in the concentrations of the metabolites and can be demonstrated by the extent of the reaction catalyzed by PFK. Because the extent of reaction of PFK moves in phase III of high [NADH] (see Fig. 6) and not in phase I, it seems that PFK switches between an active state at low [ATP] and a passive (or low rate) one at high [ATP] or low [NADH]. Superficially, the enzyme may be considered to act as an on/off switch that is flipped at the upward and downward steps of [NADH]. In the following paragraphs, the processes in the phases I–IV will be discussed.

During the OFF-state of PFK (phase I in Fig. 5), the FBP-pools is emptied by the lower part of the glycolysis path to generate ATP. The rate of this process is controlled by the consumption of ATP in other reactions. According to the scheme in Fig. 6, the hexokinase and polysaccharide synthetase reactions are the major ATP consumers. From Fig. 5 *b* in phase I, the rate of turnover in the lower glycolytic pathway is estimated to 0.28 μmol FBP/ml/min (see Results) which yields ATP at a rate of 4 × 0.28 = 1.12 μmol/ml/min. The input of glucose 0.83 μmol/ml/min is divided into one part which is built into a polysaccharide at a rate of 0.37 μmol glucose/ml/min and another part that increases the glucose-6-phosphate pool at a rate of 0.46 μmol glucose/ml/min. The rate at which ATP is consumed by the two processes, is 0.46 + 2 × 0.37 = 1.10 μmol/ml/min. The ATP generated in the lower pathway of glycolysis is consumed in the upper pathway to form the polysaccharide and fill up the glucose-6-phosphate pool. Because the production of FBP by PFK is inhibited, the FBP pool is largely drained. This state ends when the FBP pool reaches a lower limit or has been exhausted. The driving force which keeps the ATP level high in this phase is probably the ATP producing lower glycolytic pathway. The pyruvate kinase reaction which is believed to operate far from equilibrium (50, 51) may be considered as a controlling element. Here, the reaction rate also might be influenced by product inhibition. During the ON state of PFK (see Fig. 5 *b* phase III), the G6P pool is converted into FBP. The characteristics of phase III is

the high rate of ATP consumption which keeps the ATP level low. According to Fig. 5, the PFK reaction dominates and converts one glucose molecule into the FBP pool by consuming the 2 ATP molecules which are generated if another glucose molecule is turned into ethanol and CO_2. The rate of FBP production by this pathway would be one half of the input rate of glucose $0.5 \times 0.83 = 0.41$ μmol/ml/min. Simultaneously, the G6P pool is transformed to FPB at a rate of 0.6 μmol G6P/ml/min + 0.18 μmol F6P/ml/min = 0.78 μmol/ml/min. Per G6P molecule converted to ethanol and CO_2, three ATP molecules are generated which may be consumed to produce FBP and the triosephosphates from G6P and F6P. Thus, a quarter of G6P is metabolized to produce the ATP that is needed to convert three quarters of G6P to FBP. The rate at which G6P is turned to FBP computes to $0.75 \times 0.78 = 0.59$ μmol/ml/min. The sum of the rates of the two processes is 0.59 + 0.41 = 1.0 μmol/ml/min which approximately is equal to the experimental rate 0.7 [EBP] + 0.2 [DHAP] = 0.9 μmol/ml/min which is read from Fig. 5 *b* for the growth of the FBP pool. The rate of turnover in the lower pathway is estimated to 0.41 + 0.19 = 0.6 μmol FBP/ml/min which is nearly twice the rate of phase I, 0.28 μmol FBP/ml/min. The mean rate of turnover should be the half of the input rate, i.e., 0.41 μmol/ml/min. The actual rate is ~0.1 μmol ml/min lower in phase I and ~0.2 higher in phase III than the mean rate which explains that phase I is longer than phase III. Whereas the rates of the nucleotide kinases (AK and UK) are negligibly small in phase I and III, they contribute in phases II and IV to the dynamics.

The ATP required in phase II to switch from the low to the high AMP state is twice the difference between its initial and the final concentration (one equivalent to decrease the ATP concentration and a second to generate the AMP by the AK reaction). Besides the adenosine nucleotide pool, the uridyl nucleotide pool simultaneously changes and supplies ATP. The total amount of ATP removed can be estimated as $2 \times 0.7 + 2 \times 0.3 = 2.0$ μmol ATP/ml (see Fig. 5). This amount is mainly used to convert G6P and F6P (1.65 μmol/ml) in this phase into the FBP pool (1.7 μmol/ml) by PFK (see Results and Figs. 3 *b* and 5 *b*).

If substrate inhibition of PFK by ATP is occurring, then it may be relieved by lowering the ATP concentration. Because the enzyme action itself decreases the ATP concentration, the process is selfaccelerating until the enzyme has converted nearly all ATP and remains in the noninhibited state, in which the rate of conversion is determined by the supply of ATP. This resembles a reaction with autocatalytic characteristics (52), governing the fast change in phase II.

In phase IV, the substrate inhibition is restored. The reason is probably that the hexose monophosphate pool has been depleted to a level at which the rate of ATP consumption no longer is dominating over that of ATP production in the lower part of glycolysis. The reversion of the nucleotide pools to the state at the beginning of phase II requires 2.0 μmol ATP/ml. Because the PFK reaction may be considered as inhibited in phase IV, this amount should be drawn from the full FBP pool. Because four ATP molecules are generated per molecule of FBP, the equivalent change in the concentration of FBP should be 0.5 μmol/ml which may be verified in Fig. 3 and Fig. 5 (see Results).

Thus, the dynamics may be described by assuming an inhibited PFK in the slow phase I of low NADH concentrations and an active PFK in the other slow phase III. In the fast phases II and IV, PFK is switched between the states by the nucleotide pools. The course of the processes seems to be evident, but the interpretation is strongly based on the mechanism of Fig. 6, which may be incomplete.

Dynamics on the limit cycle

The dynamics on the limit cycle of Fig. 8 are usually described by two differential equations for the phase plane variables [G6P] and [ATP]. From the scheme of Fig. 6, their variation in time is given by the kinetic rate laws:

$$\frac{d}{dt}[\text{G6P}] = V_{\text{HEX}} - V_{\text{PGM}} - V_{\text{PGI}}$$

$$\frac{d}{dt}[\text{ATP}] = V_{\text{PK}} + V_{\text{PGK}} - V_{\text{PFK}} - V_{\text{HEX}} - V_{\text{AK}} - V_{\text{UK}},$$

where V is the rate of the reaction catalyzed by the enzyme given as index.

Under the experimental conditions used, some reactions move in concert (i.e., their extents of reaction advance simultaneously; see Fig. 7). The equation system above may be simplified if the rates are approximated by the rates of the rate-determining steps, i.e.:

$$V_{\text{HEX}} = V_{\text{in}};\ V_{\text{PGK}} = V_{\text{PK}};\ V_{\text{UT}} = V_{\text{SYN}} - V_{\text{UK}};$$
$$V_{\text{PGI}} = V_{\text{PFK}},\ V_{\text{PGM}} = V_{\text{SYN}} \text{ and } V_{\text{UK}} = \alpha \cdot V_{\text{AK}};$$

where V_{in} is the injection rate of glucose, V_{UT} is the rate of uridyl phosphotransferase, and α is a constant. The approximated differential equation system:

$$\frac{d}{dt}[\text{G6P}] = V_{\text{in}} - V_{\text{SYN}} - V_{\text{PFK}}$$

$$\frac{d}{dt}[\text{ATP}] = -V_{\text{in}} - V_{\text{SYN}} - V_{\text{PFK}} + 2V_{\text{PK}} - (1 + \alpha)V_{\text{AK}}$$

has as isoclines the two functions, f_1 and f_2. Their time derivatives are zero:

$$0 = f_1([G6P], [ATP]) = V_{in} - V_{SYN} - V_{PFK}$$
$$0 = f_2([G6P], [ATP]) = -V_{in} - V_{SYN} - V_{PFK} + 2V_{PK} - (1 + \alpha)V_{AK}.$$

These functions or isoclines are tentatively drawn in Fig. 8 within the limit cycle (52). The exact functions are obtained from the rate laws: V as a function of [G6P] and [ATP]. The enzyme kinetics has to be studied in detail and compared with the rates obtained from the oscillatory state to prove that the proposed dynamics are correct.

In the sector in which the isocline for $d[ATP]/dt \approx 0$ approaches the limit cycle (phase I and III), the dynamics are given by the differential equation

$$\frac{d[G6P]}{dt} = 2 \times V_{in} - 2 \times V_{PK} + (1 + \alpha) \times V_{AK}.$$

Because $V_{AK} \sim 0$ in phases I and III, this term may be neglected in the above equation. The dynamics in phases I and III are controlled by the rate in the lower glycolytic pathway V_{PK}. At high [ATP], the inactive phosphofructokinase reaction requires that the synthetase controls the rate V_{PK} and at low [ATP], the active phosphofructokinase determines V_{PK}. In the phases of fast changing metabolites II and IV, the rate of the myokinase reaction cannot be neglected and may influence the dynamics.

Remarks

The interpretation of the experimental data strongly depends on the assumptions of the mechanisms of the reactions (see Fig. 6). There may be additional reactions (e.g., the sidepath to glycerol) which have to be considered in a detailed description. Particularly, the regulation in the basic scheme of Fig. 6 may have to be extended by additional reactions. Therefore, this interpretation should not be considered as final. Experimental data (e.g., of NMR spectra [53] on the oscillatory state of glycolysis) may improve the current insight into the dynamics. The origin of the constant value of ADP in the two slowly varying phases (I and III) and that of the almost constant value of 3–4 μmol/ml for the maximal G-6-P concentration (54) await further investigation.

The steady support and encouragement of Prof. Dr. B. Havsteen during the period of this work is gratefully acknowledged. For advice and many discussions we wish to thank Prof. Dr. H. Degn, Dr. H. Jacobsen, and H. Timm.

Received for publication 13 June 1990 and in final form 1 March 1991.

REFERENCES

1. Chance, B., G. Williamson, I. Y. Lee, L. Mela, D. DeVault, A. Ghosh, and E. K. Pye. 1973. Synchronization phenomena in oscillations of yeast cells and isolated mitochondria. *In* Biological and Biochemical Oscillators. B. Chance, E. K. Pye, A. K. Ghosh, and B. Hess, editors. Academic Press, New York/London. 285–300.
2. Hommes, F. A. 1964. Oscillatory reductions of pyridine nucleotides during anaerobic glycolysis in brewer's yeast. *Arch Biochem. Biophys.* 108:36–46.
3. Ibsen, K. H., and K. W. Schiller. 1967. Oscillations of nucleotides and glycolytic intermediates in aerobic suspensions of Ehrlich ascites tumor cells. *Biochem. Biophys. Acta.* 131:405–407.
4. Kreuzberg, K., and W. Martin. 1984. Oscillatory starch degradation and fermentation in the green alga *Chlamydomonas reinhardii. Biochim. Biophys. Acta.* 799:291–297.
5. Chance, B., J. R. Williamson, D. Jamieson, and B. Schoener. 1965. Properties and kinetics of reduced pyridine nucleotide fluorescence of the isolated and in vivo rat heart. *Biochem. Z.* 341:357–377.
6. Chance, B., B. Hess, and A. Betz. 1964. DPNH oscillations in a cell-free extract of *S. carlsbergensis. Biochim. Biophys. Res. Commun.* 16:182–187.
7. Frenkel, R. 1968. Control of reduced diphosphopyridine nucleotide oscillations in beef heart extracts. II. Oscillations of glycolytic intermediates and adenine nucleotides. *Arch. Biochem. Biophys.* 125:157–165.
8. Tornheim, K. 1988. Fructose 2,6-bisphosphate and glycolytic oscillations in skeletal muscle extracts. *J. Biol. Chem.* 263:2619–2624.
9. Horning, M., and K. G. Collatz. 1990. First description of the glycolytic oscillator of an insect, the blowfly *Phormia terranovae. Comp. Biochem. Physiol.* 95B:613–618.
10. Hess, B., and A. Boiteux. 1971. Oscillatory phenomena in biochemistry. *Annu. Rev. Biochem.* 40:237–258.
11. Rapp, P. E. 1979. An atlas of cellular oscillations. *J. Exp. Biol.* 81:281–306.
12. Chance, B., K. Pye, and J. Higgins, 1967. Waveform generation by enzymatic oscillators. *IEEE spectrum.* August:79–86.
13. Pye, E. K. 1969. Biochemical mechanism underlying the metabolic oscillations in yeast. *Can. J. Botany.* 47:271–285.
14. Betz, A., and B. Chance. 1965. Phase relationships of glycolytic intermediates in yeast cells with oscillatory metabolic control. *Arch. Biochem. Biophys.* 109:585–594.
15. Das, J., H.-G. Busse, and B. H. Havsteen. 1979. Evidence for oscillations of relaxation type in glycolyzing yeast extracts. *In* Kinetics of Physicochemical Oscillations. U. F. Frank and E. Wicke, editors. Fotodruck Mainz, Aachen, FRG. 2:329–336.
16. Lavenda, B., G. Nicolis, and M. Herschkowitz-Kaufman. 1971. Chemical instabilities and relaxation oscillations. *J. Theor. Biol.* 32:283–292.
17. Boiteux A., B. Hess, and E. E. Sel'kov. 1980. Creative functions of instability and oscillations in metabolic systems. *In* Current Topics in Cellular Regulation. B. L. Horecker and E. R. Stadman, editors. Academic Press, New York. 17:171–203.
18. Swenson, K. I., K. M. Farell, and J. V. Ruderman. 1986. The clam embryo protein cyclin A induces entry into M phase and the resumption of meiosis in *Xenopus oocytes. Cell.* 47:861–870.
19. Gerhart, J., M. Wu, and M. Kirschner. 1986. Cell cycle dynamics of

an M-phase-specific cytoplasmic factor in *Xenopus laevis* oocytes and eggs. *J. Cell Biol.* 98:1247–1255.

20. Jacobsen, H., H. G. Busse, and B. H. Havsteen. 1982. Spontaneous spatiotemporal organization in yeast extracts. *J. Biol. Chem.* 257:4001–4006.
21. Weaver, J. C., and R. D. Astumian. 1990. The response of living cells to very weak electric fields: the thermal noise limit. *Science (Wash. DC).* 247:459–462.
22. Li, Y. X., and A. Goldbeter. 1989. Frequency specificity in intercellular communication. *Biophys. J.* 55:125–145.
23. Ross, J., and M. Schell. 1987. Thermodynamic efficiency in nonlinear biochemical reactions. *Annu. Rev. Biophys. Chem.* 16:401–422.
24. Rapp, P. E. 1987. Why are so many biological systems periodic? *Prog Neurobiol.* 29:261–273.
25. Estabrook, R. W., and P. K. Maitra. 1962. A fluorimetric method for the quantitative microanalysis of adenine and pyridine nucleotides. *Anal. Biochem.* 3:369–382.
26. Jaworek, D., W. Gruber, and H. U. Bergmeyer. 1974. Adenosin-5'-triphosphat—Bestimmung mit 3-Phosphoglycerat-Kinase. *In* Methoden der Enzymatischen Analyse. 3rd ed. H. U. Bergmeyer, editor. Verlag-Chemie, Weinheim, FRG. 2:2147–2151.
27. Michal, G., and H. O. Beutler. 1974. D-Fructose-1,6-diphosphat, Dihydroxyaceton-phosphat und D-glycerin-aldehyd-3-phosphat. *In* Methoden der Enzymatischen Analyse. 3rd ed. H. U. Bergmeyer, editor. Verlag Chemie, Weinheim, FRG. 2:1359–1364.
28. Czok, R. 1974. D-Glycerat-3-phosphat. *In* Methoden der Enzymatischen Analyse. 3rd ed. H. U. Bergmeyer, editor. Verlag Chemie, Weinheim, FRG. 2:1469–1473.
29. Bergmeyer, H. U., E. Bernt, F. Schmidt, and H. Stork. 1974. D-Glukose-Bestimmung mit Hexokinase und Glucose-6-phosphat-Dehydrogenase. *In* Methoden der Enzymatischen Analyse. 3rd ed. H. U. Bergmeyer, editor, Verlag Chemie, Weinheim, FRG. 2:1241–1246.
30. Lang, G., and G. Michal, G. 1974. D-Glucose-6-phosphat und D-Fructose-6-phosphat. *In* Methoden der Enzymatischen Analyse. Verlag Chemie, 3rd ed. H. U. Bergmeyer, editor. Weinheim, FRG. 2:1283–1287.
31. Das, J. 1979. Relaxationsoszillationen in cytoplasmatischen extrakten der Hefe *Saccharomyces uvarum.* PhD. thesis. Christian-Albrechts-Universität, Kiel, Germany.
32. Sander, B. J., F. J. Oelshlegel, and G. J. Brewer. 1976. Quantitative analysis of pyridine nucleotides in red blood cells: a single step extraction procedure. *Anal. Biochem.* 71:29–36.
33. Alt, J., K. Krisch, and P. Hirsch, P. 1975. Isolation of an inducible amidase from *Pseudomonas acidivorans* AE 1. *J. Gen. Microbiol.* 87:260–272.
34. Jacobsen, H. 1979. Glycolytische Oszillation und räumliche Organisation in Zellsuspensionen und Extrakten der Hefe *Saccharomyces uvarum.* PhD thesis. Christian-Albrechts-Universität, Kiel, FRG.
35. Das, J., and H.-G. Busse. 1985. Long term oscillation in glycolysis. *J. Biochem.* 97:719–727.
36. Hess, B., and A. Boiteux. 1968. Mechanism of glycolytic oscillations in yeast, I: Aerobic and anaerobic growth conditions for obtaining glycolytic oscillation. *Hoppe-Seyler's Z. Physiol. Chem.* 349:1567–1574.
37. Pye, K. 1966. Metabolic control phenomena associated with oscillatory reactions. *Stud. Biophys. (Berl.)* 1:a75–a78.
38. Chance, B., B. Schoener, and S. Elsaesser. 1965. Metabolic control phenomena involved in damped sinusoidal oscillation of reduced diphosphopyridine nucleotides in a cell-free extract of *Saccharomyces carlsbergensis. J. Biol. Chem.* 240:3170–3181.
39. Boiteux, A., A. Goldbeter, and B. Hess, B. 1975. Control of oscillating glycolysis of yeast by stochastic, periodic, and steady source of substrate: a model and experimental study. *Proc. Natl. Acad. Sci. USA.* 72:3829–3833.
40. Boiteux, A., and H.-G. Busse. 1989. Circuit analysis of the oscillatory state in glycolysis. *BioSystems.* 22:231–240.
41. Knott G. 1984. MLAB—An on-line modelling laboratory. National Institute of Health, Bethesda, MD.
42. Das, J., and H.-G. Busse. 1990. Analysis of the adenine nucleotide pool in an oscillating extract of yeast *Saccharomyces uvarum. In* Complexity, Chaos and Biological Evolution. Mosekilde, E., editor. Plenum Publishing Corporation, New York (in press).
43. Timm, H. 1989. Untersuchungen zur Metabolisierung eines substrates bei der oszillierenden Glykolyse in Hefeextrakten. Masters thesis. Kiel, FRG.
44. Das, J., H. Timm, H.-G. Busse, and H. Degn. 1990. Oscillatory CO_2 evolution in glycolysing yeast extracts. *Yeast.* 6:255–261.
45. v. Klitzing, L. 1976. Oscillatory controlled glycolysis in yeast cells—an extended model of glycolytic regulation. *Stud. Biophys.* 55:211–216.
46. Pye, E. K. 1973. Glycolytic oscillations in cells and extracts of yeast—some unsolved problems. *In* Biological and Biochemical Oscillators. Chance, B., E. K. Pye, A. K. Gosh, and B. Hess, editors. Academic Press, New York. 269–284.
47. Ratliff, R. L., R. H. Weaver, H. A. Lardy, and S. A. Kuby. 1964. Nucleoside triphosphate-nucleoside diphosphate transphosphorylase. *J. Biol. Chem.* 239:301–309.
48. Ahlfors, C. E., and T. E. Mansour. 1969. Studies on heart phosphofructokinase—desensitization of the enzyme to adenosine triphosphate inhibition. *J. Biol. Chem.* 244:1247–1251.
49. Frenkel, R. 1968. Control of reduced diphosphopyridine nucleotide oscillations in beef heart extracts. III. Purification and kinetics of beef heart phosphofructokinase. *Arch. Biochem. Biophys.* 125:166–174.
50. Ghosh, A., and B. Chance. 1964. Oscillations of glycolytic intermediates in yeast cells. *Biochem. Biophys. Res. Commun.* 16:174–181.
51. Hess, B., A. Boiteux, and J. Krüger. 1969. Cooperation of glycolytic enzymes. *Adv. Enzyme Regul.* 7:149–167.
52. Geiseler, W. 1974. Erregungsphysiologische Phaenomene an auslösbaren und periodischen chemischen Reaktionen. PhD thesis. RTWH Aachen, FRG.
53. Campell-Burk, S. L., J. A. Den Hollander, J. R. Alger, and R. G. Shulman. 1987. 31-P NMR saturation-transfer and 13-C NMR kinetic studies of glycolytic regulation. *Biochemistry.* 26:7493–7500.
54. Jonnalagadda, S. B., J. U. Becker, E. E. Sel'kov, and A. Betz. 1982. Flux regulation in glycogen-induced oscillatory glycolysis in cell-free extracts of *Saccharomyces carlsbergensis. Biosystems.* 15:49–58.